of complex isomeric mixtures and for the characterization of such reaction products.

Acknowledgment. H.K. and R.v.E. gratefully acknowledge financial support from the Deutsche Forschungsgemeinschaft, the Fonds der Chemischen Industrie, and the Max Buchner Forschungsstiftung. They also appreciate the kind assistance of Dr. G. Zimmermann (University of Frankfurt) with some of the NMR work.

Registry No. hfac, 1522-22-1; $[Co(en)_2(hfac)](ClO_4)_2$, 69496-10-2; $Co(en)_2(hfac)^{2+}$, 69496-09-9; $[Co(NH_3)_4(hfac)](ClO_4)_2$, 94090-17-2; $Co(NH_3)_4(hfac)^{2+}$, 94090-16-1; α-$[Co(trien)(hfac)](ClO_4)_2$, 94090-19-4; α-$Co(trien)(hfac)^{2+}$, 94090-23-0; β-$[Co(trien)(hfac)](ClO_4)_2$, 94233-40-6; β-$Co(trien)(hfac)^{2+}$, 94160-59-5; *fac*(*N*)-$[Co(i\text{-}dtma)(hfac)]ClO_4$, 94090-21-8; *fac*(*N*)-$Co(i\text{-}dtma)(hfac)^+$, 94090-20-7; *mer*(*N*)-$[Co(i\text{-}dtma)(hfac)]ClO_4$, 94233-41-7; *mer*(*N*)-$Co(i\text{-}dtma)(hfac)^+$, 94160-60-8; α-$[Co(edda)(hfac)]$, 94090-22-9; β-$[Co(edda)(hfac)]$, 94198-89-7; *fac*(*N*)-$[Co(i\text{-}dtma)(H_2O)_2](ClO_4)_2$, 94160-58-4; α-$[Co(edda)(H_2O)_2]ClO_4$, 32715-40-5.

Contribution from the Department of Chemistry, The Worcester Polytechnic Institute, Worcester, Massachusetts 01609

Axial Labilization by Macrocyclic Ligands. 4. Further Studies of Axial Substitution in Low-Spin Iron(II) Complexes Containing 14-Membered Tetraaza Macrocyclic Ligands

N. K. KILDAHL,* G. ANTONOPOULOS, N. E. FORTIER, and W. D. HOBEY

Received March 6, 1984

The results of studies of the kinetics of reactions 1 and 2 in acetone solvent are presented. Here, L is any of five tetraaza–tetraimine

$$FeL^2(An)_2^{2+} + 2MeIm \rightarrow FeL^2(MeIm)_2^{2+} + 2An \quad (1)$$

$$FeL(MeIm)_2^{2+} + An \rightarrow FeL(MeIm)(An)^{2+} + MeIm \quad (2)$$

macrocyclic ligands and L^2 = a specific one of these ligands, An = acetonitrile, and MeIm = *N*-methylimidazole. The limiting first-order rate constant for reaction 1, determined under pseudoorder conditions with use of the usual integrated first-order rate expression, is 24 s^{-1} at 30 °C. Limiting first-order rate constants for reaction 2, determined by the method of initial rates, range from 6.1×10^{-3} to 2.1×10^{-1} s^{-1} at 30 °C, depending upon the identity of the macrocyclic ligand, L. The results indicate that the substitutions occur via the dissociative (D) mechanism. The dissociative rate and activation parameters (obtained from the temperature dependence of the limiting first-order rate constants) vary with the structure of the macrocyclic ligand in a manner consistent with our previous findings.

Axial ligand substitution reactions of metal ions in macrocyclic ligand environments have engendered much study, since they are obviously relevant to bioinorganic systems incorporating a metal–porphyrin moiety.[1-12] We have been particularly interested in the relationship between the structure of a macrocyclic ring system and its ability to labilize the axial sites of the metal ion. We have attempted to examine this relationship in three previous papers, in which we have reported the results of studies of the kinetics of substitution of axial acetonitrile by *N*-methylimidazole in a variety of low-spin, synthetic macrocyclic ligand complexes of iron(II).[10-12] The reactions investigated are indicated in general form in reaction 1 (L = any of six macrocyclic ligands,[10-12] An = acetonitrile, and S = solvent = acetone). Herein, we report

$$FeL(An)_2^{2+} + 2MeIm \xrightarrow{S} FeL(MeIm)_2^{2+} + 2An \quad (1)$$

the results of one additional study of this type, involving the macrocyclic ligand L^2.[13] In addition, we report the results of kinetics studies of reaction 2, for all systems indicated. As for

$$FeL(MeIm)_2^{2+} + An \xrightarrow{\text{acetone}} FeL(MeIm)(An)^{2+} + MeIm \quad (2)$$

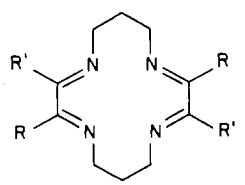

L	R	R′
L^1	CH_3	CH_3
L^2	CH_3	Ph
L^3	*p*-MeOPh	*p*-MeOPh
L^4	*p*-MePh	*p*-MePh
L^5	Ph	Ph

the previously investigated systems, reactions 1 and 2 proceed by the dissociative (D) mechanism. Dissociative rate constants and the associated activation parameters, ΔH^* and ΔS^*, are correlated with the donor ability of the macrocyclic ligand, as represented quantitatively by $E_{1/2}(Fe^{II}-Fe^{III})$, the half-wave redox potential for the reduction of Fe(III) to Fe(II) in the appropriate series of complexes.

Experimental Section

Reagents. Reagent grade acetonitrile, acetone, and *N*-methylimidazole were dried and/or purified as previously described.[10,11] All other materials were reagent grade and were used without further purification.

Syntheses. $FeL^1(An)_2(PF_6)_2$[14] and $FeL^2(An)_2(PF_6)_2$[15] were synthesized according to literature methods. $FeL(An)_2(PF_6)_2$, L = L^3–L^5, were synthesized as described previously.[10,11]

(1) Jones, J. G.; Twigg, M. V. *J. Chem. Soc., Dalton Trans.* **1978**, 1709.
(2) Holloway, C. E.; Stynes, D. V.; Viuk, C. P. *J. Chem. Soc., Dalton Trans.* **1979**, 124.
(3) Pomposo, F.; Stynes, D. V.; Hui, Y. S.; Chew, V. *Inorg. Chem.* **1982**, *21*, 1222.
(4) Pomposo, F.; Stynes, D. V. *Inorg. Chem.* **1983**, *22*, 569
(5) Martinsen, J.; Miller, M.; Trojan, D.; Sweigart, D. A. *Inorg. Chem.* **1980**, *19*, 2162.
(6) Doeff, M. M.; Sweigart, D. A. *Inorg. Chem.* **1982**, *21*, 3699.
(7) Doeff, M. M.; Sweigart, D. A. *Inorg. Chem.* **1981**, *20*, 1683.
(8) Ashley, K. R.; Shyu, S. B.; Leipoldt, J. G. *Inorg. Chem.* **1980**, *19*, 1613.
(9) Ashley, K. R.; Leipoldt, J. G. *Inorg. Chem.* **1981**, *20*, 2326.
(10) Hamilton, D. E.; Lewis, T. J.; Kildahl, N. K. *Inorg. Chem.* **1979**, *18*, 3364.
(11) Kildahl, N. K.; Lewis, T. J.; Antonopoulos, G. *Inorg. Chem.* **1981**, *20*, 3952.
(12) Kildahl, N. K.; Balkus, K. J.; Jr.; Flynn, M. J. *Inorg. Chem.* **1983**, *22*, 589.
(13) Note that we have renumbered the macrocyclic ligands to correspond more closely with their donor abilities. This should be kept in mind when comparing results in this paper with those in ref 10–12.
(14) Baldwin, D.; Pfeiffer, R. M.; Reichgott, D. W.; Rose, N. J. *J. Am. Chem. Soc.* **1973**, *95*, 5152.
(15) Eggleston, D. S.; Jackels, S. C. *Inorg. Chem.* **1980**, *19*, 1593.

0020-1669/85/1324-0429$01.50/0

Table I. Electronic Spectral Data for the Complexes $FeL(An)_2^{2+}$ and $FeL(MeIm)_2^{2+}$ [a]

L	axial ligand	λ_{max}, nm (ϵ)
L^1	An	551 (9.02×10^3), 514 (sh)
	MeIm	664 (8.9×10^3), 612 (sh)
L^2	An	571 (13.2×10^3), 532 (sh)
	MeIm	688 (13.6×10^3), 635 (sh)
L^3	An	598 (18.7×10^3), 554 (sh)
	MeIm	713 (23.6×10^3), 658 (sh)
L^4	An	584 (21.5×10^3), 543 (sh)[17]
	MeIm	710 (18.4×10^3), 655 (sh)
L^5	An	588 (16.5×10^3), 546 (sh)
	MeIm	709 (18.0×10^3), 653 (sh)

[a] Kinetics studies were performed at the long-wavelength absorption maximum in all cases.

The compounds $FeL(MeIm)_2(PF_6)_2$, L = L^1–L^5, were synthesized according to the following general procedure. $[FeL(An)_2](PF_6)_2$ (0.30 g) was dissolved in a mixture of 0.5 mL of acetonitrile and 75 mL of acetone. The solution was stirred for 10 min to ensure complete dissolution, and then a 10-fold molar excess (~0.5 mL) of MeIm was added. The solution immediately turned green-blue. After the mixture was stirred for 10 min, a small aliquot of solution was diluted with acetone and its visible spectrum was monitored for 15 min. In all cases, the spectrum was time stable and consistent with the expected spectrum of $FeL(MeIm)_2^{2+}$. The reaction solution was then filtered, and diethyl ether was added dropwise to the filtrate to precipitate the product. The blue-green precipitate was isolated by filtration, washed three times with ether, and air-dried. The product was recrystallized from acetone with addition of ether, washed with ether, and dried.

The compounds $FeL(MeIm)_2(PF_6)_2$ were characterized by IR spectroscopy and electronic absorption spectroscopy (Table I).

Physical Methods. Electronic absorption spectra were obtained with either a Perkin-Elmer 553 spectrophotometer coupled with a Perkin-Elmer R100 recorder or a Perkin-Elmer 320 spectrophotometer. IR spectra were obtained from KBr pellets with a Perkin-Elmer 683 infrared spectrometer. Cyclic voltammetry was performed in acetone solvent containing 0.1 M tetrabutylammonium perchlorate for the series $FeL(MeIm)_2^{2+}$ and in acetonitrile solvent, again containing 0.1 M TBAP, for $FeL^2(An)_2^{2+}$. Measurements were performed at a platinum-button electrode with a PAR Model 373 potentiostat–galvanostat with a PAR Model 175 universal programmer and a Houston Instruments 2000 X-Y recorder. Voltages were measured against the aqueous saturated calomel electrode (SCE). Ligand substitution kinetics were studied with either the PE 553 spectrophotometer or a HiTech SF-3A Canterbury stopped-flow system interfaced with a Digital Equipment Corp. MINC-23 microcomputer system. Low temperatures for stopped-flow studies were achieved by circulating coolant from a Neslab ULT-80 low-temperature bath/circulator through a heat exchanger submerged in the thermostating bath for the stopped-flow system. Low temperatures for conventional spectrophotometric kinetics studies were achieved by circulating coolant from a Forma Masterline Model 2800 constant-temperature bath through the cell block of the PE 553. To avoid interference by water and oxygen, all solutions for the kinetics studies were prepared under N_2 atmosphere in a Vacuum Atmospheres HE 43-2 Dri-Lab equipped with a MO-40-IV Dri-Train, and all stopped-flow studies were carried out under 1 atm of N_2. Due to the nature of the conventional spectrophotometric kinetic studies, strict maintenance of N_2 atmosphere was difficult; however, exposure of the reactant solutions to atmospheric moisture and O_2 was minimized. Reaction 1 was studied under pseudoorder conditions in iron reactant. The appearance of $FeL^2(MeIm)_2^{2+}$ was monitored at 688 nm. For reaction 2, the disappearance of $FeL(MeIm)_2^{2+}$ was monitored at the appropriate λ_{max} value (see Table I). Initial rate constants were measured for reaction 2 in all cases (vide infra).

Results

Characterization of New Complexes. Electronic absorption spectral data for new complexes, $FeL(MeIm)_2(PF_6)_2$, are reported in Table I. To facilitate comparisons, electronic spectral data for the bis(acetonitrile) complexes are also reported in Table I.

Kinetics Studies. Reaction 1, L = L^2. (All concentrations given hereafter are those that prevail after mixing of reactant solutions in either the stopped-flow mixing cell or the 1-cm cell used for standard spectrophotometric studies.) The kinetics of reaction 1, L = L^2, were followed at 9.5 °C by the stopped-flow method under nitrogen atmosphere by monitoring the appearance of

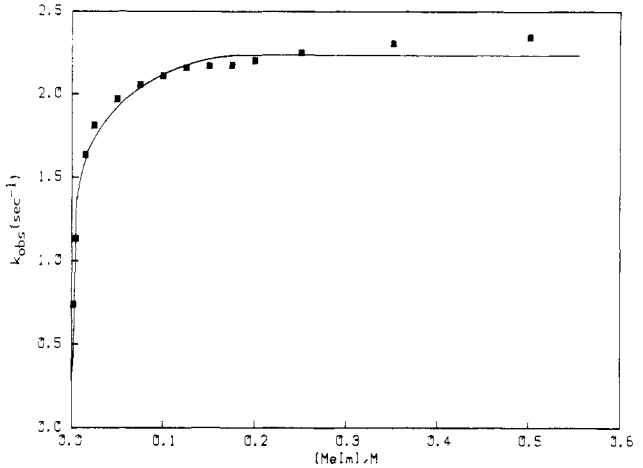

Figure 1. Dependence of k_{obsd} on [MeIm] for reaction 1, L = L^2 ([An] = 0.115 M; [Fe] = 7.5×10^{-5} M; T = 9.5 °C).

$FeL^2(MeIm)_2^{2+}$ at 688 nm. Iron concentrations of 7.5×10^{-5} M were used. The reaction is first order in iron, as shown by strict linearity, over several half-lives, of plots of ln $(A_\infty - A)$ vs. t. Here A is the absorbance of the solution at time t, and A_∞ is the absorbance at equilibrium. The slopes of such plots yield pseudo-first-order rate constants, k_{obsd}, according to the standard integrated first-order rate law.[16]

The dependence of k_{obsd} on the concentration of incoming ligand (MeIm) at a fixed An concentration of 0.115 M (a value sufficient to prevent replacement of axial An by solvent molecules, as determined by spectrophotometric titration) is shown in Figure 1. At MeIm concentrations >0.12 M, the value of k_{obsd} becomes essentially independent of [MeIm], and the reaction reaches a limiting rate of 2.23 ± 0.07 s^{-1} (the mean value of k_{obsd} for [MeIm] > 0.12 M) at 9.5 °C. (The small increase in k_{obsd} with increasing [MeIm] at [MeIm] > 0.12 M may indicate that the limiting rate has not been quite achieved. On the other hand, the scatter in the data is well within the 5–10% uncertainty in measured values of k_{obsd}. This realization and the behavior of previously studied systems lead us to believe that k_{obsd} is essentially constant above 0.12 M MeIm.) We have shown previously that axial ligand substitution processes of low-spin $FeL(An)_2^{2+}$-type complexes proceed by the D mechanism in eq 3–5 (charges omitted for

$$FeL(An)_2 + MeIm \rightleftarrows FeL(An)(MeIm) + An \quad K, \text{ rapid} \tag{3}$$

$$FeL(An)(MeIm) \rightleftarrows FeL(MeIm) + An \quad k_{-An}, k_{An} \tag{4}$$

$$FeL(MeIm) + MeIm \rightarrow FeL(MeIm)_2 \quad k_{MeIm} \tag{5}$$

clarity. Under conditions of low [An] and high [MeIm], the full rate law for this mechanism reduces to eq 6, where $[Fe]_T$ =

$$\text{rate} = k_{-An}[Fe]_T \tag{6}$$

$[FeL(An)_2] + [FeL(An)(MeIm)]$. The value of k_{obsd} is thus a direct measured of k_{-An} in the limiting-rate region of the k_{obsd} vs. [MeIm] profile, allowing us to conclude that k_{-An} for the $FeL^2(An)_2^{2+}$ system has the value 2.23 s^{-1} at 9.5 °C.

We have previously discussed the significance of the dissociative rate constant, k_{-An}, and the corresponding activation parameters, ΔH^* and ΔS^*, in the context of our general program of study of axial labilization by macrocyclic ligands.[10] To determine the activation parameters for the L^2 system, we performed temperature studies of reaction 1 under limiting-rate conditions between 0 and 30 °C. The activation parameters derived from these studies are ΔH^* = 79.5 ± 2.5 kJ/mol and ΔS^* = 44.0 ± 8.8 J/(mol K). The value of k_{-An} at 30 °C, calculated from the Eyring equation, is 23.6 s^{-1}. These results are given in Table II, along with those for the systems L^1 and L^3–L^5.

(16) Frost, A. A.; Pearson, R. G. "Kinetics and Mechanism", 2nd ed.; Wiley: New York, 1961.

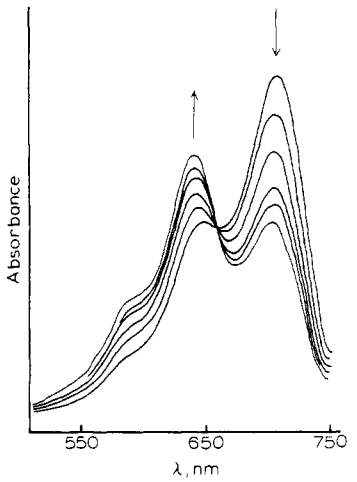

Figure 2. Spectral changes following addition of 0.5 mL of 9.57 M An in acetone to 3.5 mL of 1×10^{-4} $FeL^5(MeIm)_2^{2+}$.

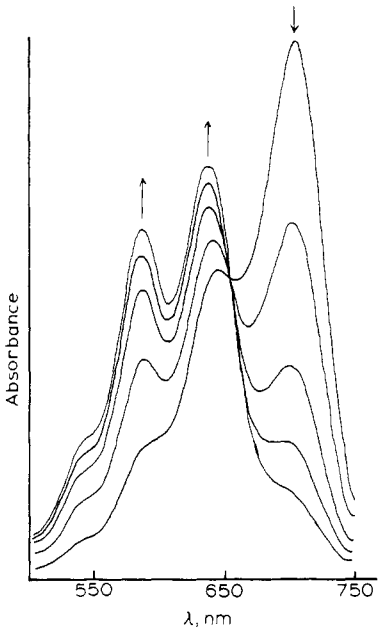

Figure 3. Spectral changes following addition of 3 mL of An to 1 mL of 4×10^{-4} M $FeL^5(MeIm)_2^{2+}$ in acetone.

Reaction 2, L = L^1–L^5. Dissolution of any of the complexes $FeL(MeIm)_2(PF_6)_2$ in dry acetone results in a blue-green solution having an absorption spectrum consistent with the data in Table I. The spectrum is time stable, indicating that the axial MeIm ligands have little or no tendency to dissociate in acetone solution, even in the absence of excess MeIm. Addition of An to such a solution results in slow color changes resulting from replacement of MeIm by An in the axial sites. Figure 2 shows a representative series of spectral scans following addition of 0.5 mL of 9.57 M An in acetone to 3.5 mL of $\sim 1 \times 10^{-4}$ M $FeL^5(MeIm)_2(PF_6)_2$. Simultaneous disappearance of the band at 709 nm (characteristic of $FeL^5(MeIm)_2(PF_6)_2$) and appearance of the band at 644 nm (characteristic of $FeL^5(An)(MeIm)$), with an isosbestic point at 655 nm, is consistent with the occurrence of reaction 2 in the solution. Clearly the reaction is incomplete, as judged from the residual absorbance at 709 nm in the equilibrium spectrum, even in the presence of 1.20 M An. Addition of sufficiently large concentrations of An results in essentially complete disappearance of $FeL^5(MeIm)_2^{2+}$ and formation of some $FeL^5(An)_2^{2+}$, as judged by the appearance of an absorption maximum at $\lambda = 588$ nm, characteristic of the bis(acetonitrile) complex. Figure 3 shows a representative series of spectra resulting from addition of 3 mL of An to 1 mL of $\sim 4 \times 10^{-4}$ M $FeL^5(MeIm)_2(PF_6)_2$ in acetone. Thus for large acetonitrile concentrations (14.4 M in this case),

Table II. Dissociative Rate and Activation Data for

$$FeL(An)_2^{2+} + 2MeIm \xrightarrow{\text{acetone}} FeL(MeIm)_2^{2+} + 2An$$

L	k_{-An}, s^{-1} (30 °C)	ln k_{-An}	ΔH^*, kJ/mol	ΔS^*, J/(mol K)	$E_{1/2}$ (Fe^{II}–Fe^{III}), V
L^1	195	5.273	67.8 ± 10.5	22 ± 36	0.97
L^2	23.6	3.161	79.5 ± 2.5	44 ± 9	1.09
L^3	14.8	2.695	81.6 ± 15.9	49 ± 27	1.12
L^4	8.5	2.140	91.2 ± 1.3	73 ± 4	1.22
L^5	4.4	1.482	90.8 ± 8.8	67 ± 29	1.25

Table III. Experimental Conditions for Kinetics Studies of Reaction 2

L	$10^4 \times$ [Fe], M	[An], M	λ, nm	T or T range, K
	k_{obsd} as a Function of [An], at Fixed Temperature			
L^2	1.58	0.75–2.50	688	308.2
L^4	0.55	0.64–2.30	710	302.8
	k_{obsd} as a Function of T, at Fixed [An]			
L^1	1.58	3.83	665	294.4–318.2
L^2	0.75	17.23	688	283.8–308.9
L^3	0.55	17.23	713	282.8–308.7
L^4	0.65	17.23	710	282.7–308.2
L^5	0.75	17.23	708	283.8–309.5

Table IV. Initial Rate Constants for the L^2 System as a Function of [An] and Temperature[a]

k_{obsd}, s^{-1}	[An], M	T, K	k_{obsd}, s^{-1}	[An], M	T, K
0.04	0.75	308	0.00148	17.23	283.8
0.0445	1.0		0.00334		289.0
0.0441	1.53		0.00633		293.6
0.0470	2.0		0.0128		298.2
0.0478	2.25		0.0253		302.8
0.0460	2.50		0.0580		308.8

[a] Conditions: [Fe] = 1.58×10^{-4} M; $\lambda = 688$ nm.

reaction 7 occurs in addition to reaction 2. However, even at such

$$FeL(MeIm)(An) + An \rightarrow FeL(An)_2 + MeIm \quad (7)$$

large concentrations of An, reaction 7 is incomplete, so that under the conditions of our studies reaction 2 is the predominant process in solution. The fact that the isosbestic point at 655 nm persists even under conditions where reaction 7 occurs indicates that equilibrium is rapidly established between $FeL(An)(MeIm)^{2+}$ and $FeL(An)_2^{2+}$ according to reaction 7, following occurrence of reaction 2. All of the systems, L^1–L^5, behave in a qualitatively similar way. Clearly, then, our measured rates (vide infra) correspond to the rate of reaction 2, and it is for this reason that we focus on this process in this paper.

Addition of enough MeIm to ensure the constancy of its concentration throughout the course of reaction completely retards both reactions 7 and 2. It was therefore not possible to study the reaction under the usual pseudoorder conditions. Consequently, we performed initial rate studies on all systems. Initial rates were calculated as the slopes at $t = 0$ of plots of absorbance vs. time, obtained by stopped-flow spectrophotometry for the L^1 system and by standard mixing and spectrophotometric techniques for the remaining systems. Experimental conditions for the five systems studied are presented in Table III, and initial rate constants for the L^2 system are given as a function of acetonitrile concentration and temperature in Table IV. It is clear from the data of Table IV that the value of k_{obsd} is independent of the acetonitrile concentration in the range between 0.75 and 2.50 M, indicating that the reaction is in the limiting rate region under these concentration conditions (a dissociative mechanism has been established for reaction 1 and is thus assumed for the first step of the reverse process, reaction 2). In fact, this rate constant

Table V. Dissociative Rate and Activation Parameters for

$$FeL(MeIm)_2^{2+} + An \xrightarrow{\text{acetone}} FeL(An)(MeIm)^{2+} + MeIm$$

L	k_{-MeIm}, s^{-1} (30 °C)	ln k_{-MeIm}	ΔH^*, kJ/mol	ΔS^*, J/(mol K)	$E_{1/2}$-(Fe^{II}–Fe^{III}), V
L^1 [a]	0.21	−1.58	82.4 ± 9.8	14 ± 32	0.550
L^2	0.025	−3.68	104.2 ± 4.3	68 ± 14	0.715
L^3	0.016	−4.15	112.2 ± 10.7	92 ± 36	0.745
L^4	0.0099	−4.62	102.9 ± 8.2	56 ± 28	0.799
L^5	0.0061	−5.10	113.3 ± 16.2	86 ± 55	0.854

[a] Data for this system obtained by stopped-flow methods.

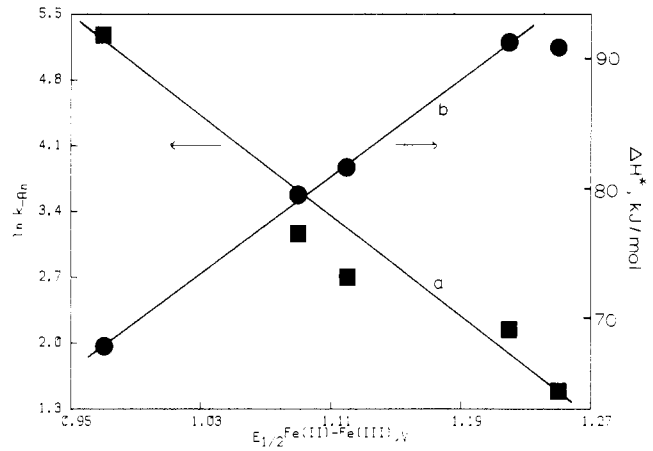

Figure 4. (a) Correlation of ln k_{-An} with $E_{1/2}(Fe^{II}–Fe^{III})$ for the FeL-$(An)_2^{2+}$–MeIm systems. (b) Correlation of ΔH^* with $E_{1/2}(Fe^{II}–Fe^{III})$ for the same systems.

remains the same for An concentrations as high as 17 M. We therefore conclude that for L = L^2, $k_{obsd} = k_{-MeIm}$, where k_{-MeIm} is the rate constant for dissociative loss of MeIm from FeL^2-$(MeIm)_2^{2+}$. For this system, then, k_{-MeIm} has the value 0.046 ± 0.002 s^{-1} at 35 °C. From the temperature dependence of k_{-MeIm}, determined with use of 16 M An to ensure the greatest accuracy in the initial rate constant, we calculate ΔH^* = 104.2 ± 4.3 kJ/mol and ΔS^* = 68 ± 14 J/(mol K). The remaining systems, L^1 and L^3–L^5, exhibit similar behavior and were studied under similar conditions. The results of temperature studies for reaction 2, L = L^1–L^5, are collected in Table V.

Cyclic Voltammetry of the $FeL(MeIm)_2^{2+}$ Systems. In all cases, well-defined, reversible redox cycles were observed for the Fe^{II}–Fe^{III} couple. The results of the electrochemical measurements were presented in Tables II and V. It should be noted that all values for $E_{1/2}(Fe^{II}–Fe^{III})$ given in these two tables were measured in our laboratory. Although some electrochemical data are available in the literature for the $FeL(An)_2^{2+}$ systems,[17] they were obtained under conditions somewhat different from ours. We felt it important to use an internally consistent set of $E_{1/2}$ values for the comparisons made in this paper.

Discussion

The results of our studies of reaction 1 are collected in Table II. It is noteworthy that for all systems ΔH^* and ΔS^* are large and positive, providing strong support for our contention that the D mechanism is operative in all cases. We have previously shown[10,11] that, for the systems L^1 and L^3–L^5, both the dissociative rate constant for axial ligand substitution according to reaction 1 and the activation enthalpy governing the temperature dependence of this rate constant correlate well with $E_{1/2}$ for the Fe^{II}–Fe^{III} couple in the complexes $FeL(An)_2^{2+}$, where $E_{1/2}$ is used as a quantitative measure of macrocyclic ligand donor ability.[18] Figure

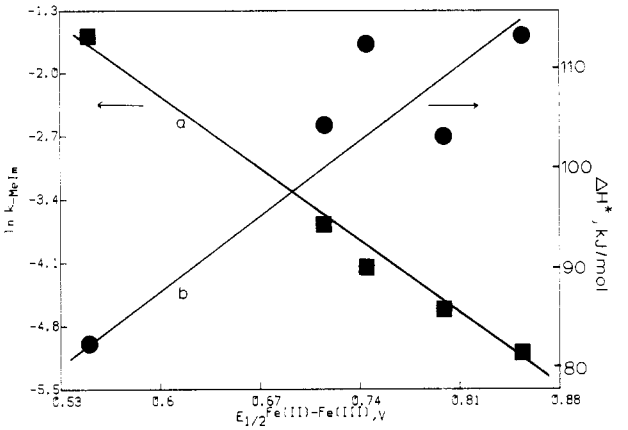

Figure 5. (a) Correlation of ln k_{-MeIm} with $E_{1/2}(Fe^{II}–Fe^{III})$ for the FeL-$(MeIm)_2^{2+}$–An systems. (b) Correlation of ΔH^* with $E_{1/2}(Fe^{II}–Fe^{III})$ for the same systems.

4a shows a plot of ln k_{-An} vs. $E_{1/2}(Fe^{II}–Fe^{III})$ for all five of the systems indicated in Table III, and Figure 4b shows the corresponding plot for ΔH^*. The L^2 system clearly fits the previously established trend, which indicates that, as the donor ability of the macrocyclic ligand increases, as reflected in a decreasing value of $E_{1/2}$, the axial ligand substitution rate increases and the activation enthalpy decreases. For reactions occurring by the D mechanism this may be interpreted in terms of decreasing metal–axial ligand bond strength with increasing in-plane donation by the macrocyclic ligand.

The results of our studies of reaction 2 are presented in Table V. We may draw several conclusions from the information in the table. First, we note that, as for reaction 1, ΔH^* and ΔS^* have large positive values for all systems, which is consistent with dissociative activation. Second, for a given macrocyclic ligand, ΔH^* is larger when MeIm is the axial ligand than when An is the axial ligand. This is expected on the basis of relative donor abilities of the two ligands. Third, again for a given macrocyclic ligand, $E_{1/2}$ for the Fe(II)–Fe(III) couple occurs at a more positive potential for $FeL(An)_2^{2+}$ than for $FeL(MeIm)_2^{2+}$. Fe(II) is clearly more readily oxidized when coordinated axially by the strongly donating MeIm than when coordinated by the weaker ligand, An. Fourth, there appears to be a qualitative correlation between the rate of axial ligand substitution and macrocycle donor ability for reaction 2. This is put on a quantitative basis in Figure 5, which shows plots of ln k_{-MeIm} (Figure 5a) and ΔH^* (Figure 5b) vs. $E_{1/2}(Fe^{II}–Fe^{III})$ for the $FeL(MeIm)_2^{2+}$ complexes. As is the case for reaction 1, correlation of ln k_{-MeIm} with $E_{1/2}$ is quite good, whereas that of ΔH^* with $E_{1/2}$ is weaker. There are two reasons for this. First, the rate constant inherently incorporates effects of both the entropy and enthalpy of activation. Since both parameters may be influenced by changes in the electron distribution in the complexes, a correlation including the effects of both might be expected to be superior to one involving enthalpy alone. Second, the error limits associated with ΔH^* are rather large, and the range of values spanned by the series is small. Despite these limitations, its seems clear from the results of our studies of reactions 1 and 2 that, for a series of complexes containing a closely related series of macrocyclic ligands, reactivity of the metal ion at the axial sites sites correlates well and understandably with macrocyclic ligand structure.

Acknowledgment. We gratefully acknowledge the National Science Foundation (Grant No. PRM8117594-CH) for support for this study.

Registry No. An, 75-05-8; MeIm, 616-47-7; $FeL^1(An)_2^{2+}$, 49861-52-1; $FeL^1(MeIm)_2^{2+}$, 59575-79-0; $FeL^2(An)_2^{2+}$, 70369-00-5; $FeL^2(MeIm)_2^{2+}$, 94070-27-6; $FeL^3(An)_2^{2+}$, 70368-96-6; $FeL^3(MeIm)_2^{2+}$, 94070-28-7; $FeL^4(An)_2^{2+}$, 70368-94-4; $FeL^4(MeIm)_2^{2+}$, 94070-29-8; $FeL^5(An)_2^{2+}$, 70369-08-3; $FeL^5(MeIm)_2^{2+}$, 94070-30-1.

(17) Goel, R. G.; Henry, P. M.; Polyzou, P. *Inorg. Chem.* **1979**, *18*, 2148.
(18) Lovecchio, F. V.; Gore, E. S.; Busch, D. H. *J. Am. Chem. Soc.* **1974**, *96*, 3109.